Faraday waves in quasi-one-dimensional superfluid Fermi-Bose mixtures

F. Kh. Abdullaev[1,2], M. Ögren[3], and M. P. Sørensen[3]
[1]*Physical - Technical Institute, Uzbek Academy of Sciences, 2-b, G. Mavlyanov str., 100084, Tashkent, Uzbekistan;*
[2]*Instituto de Fisica Teorica, UNESP, R. Dr. Bento Teobaldo Ferraz, 271, Barra Funda, Sao Paulo-SP CEP 01140-070, Brasil;*
[3]*Department of Mathematics, Technical University of Denmark, 2800 Kgs. Lyngby, Denmark*
(Dated: November 27, 2012)

Generation of Faraday waves in superfluid Fermi-Bose mixtures in elongated traps is investigated. The generation of waves is achieved by periodically changing a parameter of the system in time. Two types of modulations of parameters are considered, first a variation of the fermion-bosons scattering length, and secondly the boson-boson scattering length. We predict the properties of the generated Faraday patterns and study the parameter regions where they can be excited.

PACS numbers: 03.75.Ss, 03.75.Kk, 05.45.-a

I. INTRODUCTION

Faraday waves (FW) are spatially periodic patterns that can be generated in a system with a periodic variation in time of the system parameters. First Faraday waves was observed by Faraday for a vessel with a liquid oscillating in the vertical direction [1]. Such type of structures can exist in nonlinear optical systems [2–6] where variations along the longitudinal direction of the Kerr nonlinearity can be achieved by the periodic variation of the effective cross-sectional area of the nonlinear optical fiber. Recently parametric resonances in modulational instability of electromagnetic waves in photonic crystal fibers with a periodically varying diameter has been experimentally observed in [7]. Other examples are the patterns in the Bose-Einstein condensates (BEC) with an atomic scattering length or a radial confinement (a transverse frequency of the trap) periodically varying in time. For BECs the cases of single [8–10] and two components condensates [11, 12], as well as dipolar condensates [13, 14], have been investigated. In BEC FW was first predicted in 2D with a periodically varying transverse frequency of the trap [8] and later observed in an experiment with a repulsive interacting BEC, loaded into an elongated trap [15]. The existence of FW also in elongated fermionic clouds was discussed in the work [16] and Faraday patterns in a superfluid Fermi gas has been investigated recently in [17].

Periodic modulation of the coefficients of nonlinearity in the relevant mean-field equations can be achieved by variation of the atomic scattering length by the Feshbach resonance technics [18–21] or by time modulation of the transverse frequency of the trap [8]. In the former case it is necessary to vary the external magnetic field in time near the resonant value. The presence of a deep optical lattice has been shown to suppress the Faraday pattern generation [22].

The purpose of this work is to investigate the mechanism of Faraday wave generation in elongated superfluid Fermi-Bose (FB) mixtures. Such FB mixtures have many interesting properties in comparison with the pure bosonic case [23] and Faraday waves can be an useful tool to measure the nonlinear properties and in particular instabilities in these systems. Two types of atomic scattering lengths are relevant in this system. First the fermion-bosons scattering length describing the scattering between fermionic and bosonic atoms a_{fb}, secondly the boson-boson scattering length a_b. Variation in time of these lengths by an external magnetic field opens up for the possibility of generating Faraday waves in the mixture. The action of these variations are different though. In the latter bosonic case we parametrically excite the BEC subsystem, while in the first case we excite the bosonic and fermionic subsystems simultaneously. Thus we can expect different responses on temporal parametric perturbation with various types of pattern formation.

Strongly repulsive interacting bosons in 1D, so called Tonks-Girardeau gases [24], have the same long-wavelength dynamics as non-interacting fermions [25]. Hence, the results presented here can also be realised in systems with two coupled bosonic species with strong/weak intra-species interactions.

II. THE MODEL

The model of a quasi-one-dimensional superfluid FB mixture is described by the following system of coupled equations for the complex functions $\psi_{1,2}(x,t)$ [23]

$$\begin{aligned} i\psi_{1,t} &= -\psi_{1,xx} + g_b|\psi_1|^2\psi_1 + g_{12}|\psi_2|^2\psi_1, \\ i\psi_{2,t} &= -\psi_{2,xx} + \kappa\pi^2|\psi_2|^4\psi_2 + g_{21}|\psi_1|^2\psi_2. \end{aligned} \quad (1)$$

In general Bose- and Fermi subsystems are described by the Lieb-Liniger and the Gaudin-Yang theories respectively. Here we are interested in weak Bose-Bose interactions (we consider small positive g_b) and attractive Fermi-Fermi interactions and the superfluid Fermi-Bose system is then described by the nonlinear Schrödinger-like-equation (1) [26–30]. In the BCS weak attractive coupling limit the fermionic subsystem coefficient is $\kappa = 1/4$, while in the molecular unitarity limit it is $\kappa = 1/16$ [23].

Finally, for the bosonic Tonks-Girardeau limit [25] with components 1 (2) being a weakly- (strongly-) repulsive bosonic species we have $\kappa = 1$. Furthermore, $g_b = 2\hbar a_b \omega_\perp$ is the 1D coefficient of mean-field nonlinearity for bosons, where a_b is the scattering length and $\omega_\perp$ is the perpendicular frequency of the trap. Similarly, g_{12} is the inter-species interaction coefficient [23]. The system is written in dimensionless form using the variables

$$l = \sqrt{\frac{\hbar}{m_b \omega_\perp}}, \psi = \sqrt{l}\Psi, t = \tau\omega_\perp, x = \frac{X}{l}, g_j = \frac{2m_b l}{\hbar^2} G_j,$$

where $G_j,\ j = b, 12$ is the coefficients of the mean-field nonlinearities. We also implicitly assume $m_b = m_f$ in (1), since such conditions can be realized approximately in the mixtures ^{7}Li - ^{6}Li and ^{39}K - ^{40}K.

Below we will consider the case of identical interaction coefficients $g_{21} = g_{12}$. The mean-field nonlinearities will be varied in time as

$$\begin{aligned} g_{12}(t) &= g_{12}^{(0)}[1 + \alpha_{12}\cos(\Omega_{12}t)], \\ g_b(t) &= g_b^{(0)}[1 + \alpha_b \cos(\Omega_b t)]. \end{aligned} \quad (2)$$

Such variation can be achieved for example by using Feshbach resonance technics, namely by variation of an external magnetic field near a resonant value [18]. This leads to the temporal variation of inter- and intra-species scattering lengths and the respective mean-field coefficients.

The system (1) has plane wave solutions

$$\psi_{1,2} = A_{1,2}\exp(i\phi_{1,2}),\ A_{1,2}\ \in \mathbb{R}^+, \quad (3)$$

where

$$\begin{aligned} \phi_1 &= -g_b A_1^2 t + g_{12} A_2^2 t, \\ \phi_2 &= -\kappa\pi^2 A_2^4 t + g_{12} A_1^2 t. \end{aligned} \quad (4)$$

III. MODULATIONAL INSTABILITY OF PLANE WAVES

Let us now study the modulational instability (MI) of nonlinear plane waves using the linear stability analysis [5]. We will look for solutions of the form

$$\psi_{1,2} = [A_{1,2} + \delta\psi_{1,2}(x,t)]\, e^{i\phi_{1,2}(t)},\ |\delta\psi_{1,2}| \ll A_{1,2}. \quad (5)$$

Substituting these expressions into the system (1) and linearizing, we get the following system for $\delta\psi_{1,2}$

$$\begin{aligned} i\delta\psi_{1,t} &- g_b(t)A_1^2(\delta\psi_1 + \delta\psi_1^*) + \delta\psi_{1,xx} \\ &+ g_{12}(t)A_1A_2(\delta\psi_2 + \delta\psi_2^*) = 0, \\ i\delta\psi_{2,t} &- 2\kappa\pi^2 A_2^4(\delta\psi_2 + \delta\psi_2^*) + \delta\psi_{2,xx} \\ &+ g_{12}(t)A_1A_2(\delta\psi_1 + \delta\psi_1^*) = 0. \end{aligned} \quad (6)$$

With $\delta\psi_1 = u + iv$ and $\delta\psi_2 = p + iq$, we use the Fourier transform in the spatial coordinate to transform Eqs. (6) into functions of the wavenumber k and the time t denoted by the corresponding capital letters. Differentiation with respect to time of the remaining differential equations containing V_t and Q_t, we get the following system

$$\begin{aligned} V(k,t)_{tt} + \omega_1^2(t)V(k,t) &= \varepsilon(t)Q(k,t), \\ Q(k,t)_{tt} + \omega_2^2 Q(k,t) &= \varepsilon(t)V(k,t), \\ U(k,t) = k^2\int dt\, V,\ P(k,t) &= k^2\int dt\, Q, \end{aligned} \quad (7)$$

where

$$\begin{aligned} \omega_1^2(t) = k^2\left[k^2 + 2g_b(t)A_1^2\right],\ \omega_2^2 &= k^2(k^2 + 4\kappa\pi^2 A_2^4), \\ \varepsilon(t) &= 2g_{12}(t)k^2 A_1 A_2. \end{aligned} \quad (8)$$

Here $g_b(t)$ and $g_{12}(t)$ are defined in Eqs. (2). In the following we use the notation $\omega_1 \equiv \omega_1(t = \pi/2\Omega_b)$ and $\varepsilon_0 \equiv \varepsilon(t = \pi/2\Omega_{12})$. Hence, by solving the coupled equations for V and Q for given k, all the components of $\delta\psi_{1,2}$ can in principle be obtained by the inverse Fourier transform.

We here first consider the case of a FB mixture with constant system parameters. Looking for solutions V and Q with a time dependence of the form $\exp(\pm i\Omega t)$, we obtain the dispersion relation of the modulations

$$\Omega_{1,2}^2 = \frac{\omega_1^2 + \omega_2^2}{2} \pm \sqrt{\frac{\left(\omega_2^2 - \omega_1^2\right)^2}{4} + \varepsilon_0^2}. \quad (9)$$

Such that in the weak coupling limit $\varepsilon_0 \ll \omega_2^2 - \omega_1^2$

$$\Omega_1^2 \to \omega_1^2 - \frac{\varepsilon_0^2}{\omega_2^2 - \omega_1^2},\ \ \Omega_2^2 \to \omega_2^2 + \frac{\varepsilon_0^2}{\omega_2^2 - \omega_1^2}, \quad (10)$$

while in the limit of approaching frequences $\omega_2 \to \omega_1$

$$\Omega_1^2 \to \omega_1^2 - \varepsilon_0,\ \ \Omega_2^2 \to \omega_2^2 + \varepsilon_0. \quad (11)$$

The stability condition (for any k) is obtained by requiring $\Omega_{1,2}$ in (9) to be real, i.e.

$$g_{12}^{(0)} < \sqrt{2\pi^2\kappa g_b^{(0)} A_2^2}. \quad (12)$$

In opposite case we have MI in the FB mixture [23].

IV. ANALYSIS OF PARAMETRICALLY EXCITED INSTABILITIES

Below we will consider the linear ODE model (7) for different cases of periodic modulations (2).

When only the inter-species interaction parameter g_{12} is modulated, we obtain a system of two coupled oscillators with a coupling parameter varying in time

$$\begin{aligned} V_{tt} + \omega_1^2 V &= \varepsilon(t)Q, \\ Q_{tt} + \omega_2^2 Q &= \varepsilon(t)V, \end{aligned} \quad (13)$$

where $\varepsilon(t) = \varepsilon_0 + \alpha_{12}\varepsilon_0\cos(\Omega_{12}t)$ according to Eq. (8).

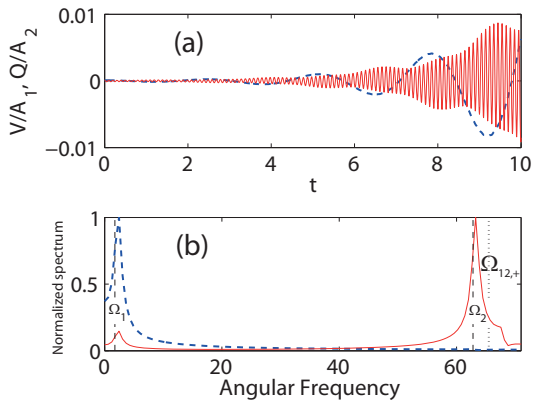

FIG. 1: (Color online) Solutions to the ODE model of Eq. (13). (a) Amplitudes growing exponentially in time. (b) Spectrum for the modulation frequency $\Omega_{12,+} = 65.5$ for the wavenumber $k = 1$ (see text) and with Ω_1 and Ω_2 from Eq. (9), which agrees well with (10) in this regime. Blue dashed curves are for V (bosons) while red thin curves are for Q (fermions). Initial conditions are $V/A_1 = Q/A_2 = 10^{-4}$ ($V_t = Q_t = 0$) and the parameters here are: $\alpha_{12} = 0.25$, $A_1 = \sqrt{300}$, $A_2 = \sqrt{20}$, $g_b^{(0)} = 0.01$, $g_{12}^{(0)} = 0.8$ and $\kappa = 1/4$.

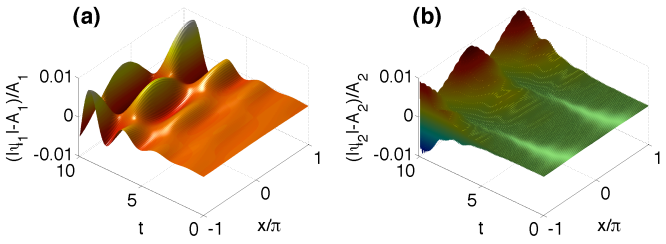

FIG. 2: (Color online) Solutions to the full PDE model of Eq. (1) for driven coupling between fermions and bosons with the modulation frequency $\Omega_{12,+} = 65.5$ ($k = 1$). We plot the oscillating parts $(|\psi_j| - A_j)/A_j$ for $j = 1$ (bosons) in (a), and for $j = 2$ (fermions) in (b). Initial conditions are $\psi_j = A_j[1 + 10^{-4}\exp(ikx)]$ and boundary conditions in x are periodic. The parameters are the same as for Fig. 1.

When only the intra-species parameter g_b is modulated, we get a system of one Mathieu equation coupled to an oscillator equation

$$\begin{aligned} V_{tt} + \omega_1^2(t)V &= \varepsilon_0 Q, \\ Q_{tt} + \omega_2^2 Q &= \varepsilon_0 V, \end{aligned} \tag{14}$$

where $\omega_1^2(t) = \omega_1^2 + \alpha_b\omega_1^2\cos(\Omega_b t)$.

A. Driven coupling between fermions and bosons

We consider the case of a stable FB mixture according to (12) such that the MI is absent [23]. Hence, any instability is only due to parametric resonance. To analyze resonances of the system (13) we use the multiscale method [31, 32]. The derivations are collected in the Appendix where we conclude that parametric resonances may occur at the two frequencies of excitations

$$\Omega_{12,-} = \omega_2 - \omega_1, \;\; \Omega_{12,+} = \omega_2 + \omega_1. \tag{15}$$

As the detailed analysis shows, the excitations for $\Omega_{12,-}$ are stable and do not lead to FW. Inserting the expressions from Eq. (8) for the second case of Eq. (15), with the use of a simplified notation $a = 2g_b^{(0)}A_1^2$ and $b = 4\pi^2\kappa A_2^4$, we get the resonance frequences in terms of the wavenumbers of the corresponding Faraday waves

$$\Omega_{12,+} = k(\sqrt{k^2 + a} + \sqrt{k^2 + b}). \tag{16}$$

We invert (16), such that the wavenumbers are

$$k^2 = \frac{a + b - 2\sqrt{ab + \Omega_{12,+}^2}}{(b-a)^2 - 4\Omega_{12,+}^2}\,\Omega_{12,+}^2. \tag{17}$$

The spatial wavelength $L = 2\pi/k$ of the FW obtained from Eq. (17) is

$$L(\Omega, \kappa) = \frac{2\pi}{\Omega_{12,+}}\sqrt{\frac{(b-a)^2 - 4\Omega_{12,+}^2}{a + b - 2\sqrt{ab + \Omega_{12,+}^2}}}. \tag{18}$$

According to the Appendix, the region of instability for $\Omega_{12,+}$ from (15) is restricted by the lines

$$\bar{\omega}_1^2 \simeq \omega_1^2 \pm \frac{\varepsilon_0\alpha_{12}}{2}\sqrt{\frac{\omega_1}{\omega_2}},\;\; \bar{\omega}_2^2 \simeq \omega_2^2 \pm \frac{\varepsilon_0\alpha_{12}}{2}\sqrt{\frac{\omega_2}{\omega_1}}, \tag{19}$$

while the exponential growth rate of the amplitudes is restricted by the maximal gain

$$p_m \simeq \frac{\varepsilon_0\alpha_{12}}{4\sqrt{\omega_1\omega_2}}. \tag{20}$$

A mathematically particularly simple case of the driven inter-species modulation is when $\omega_1 \simeq \omega_2$. Introducing the symmetric $[\xi_+(t) = (V + Q)/2)]$ and antisymmetric $[\xi_-(t) = (V - Q)/2]$ combinations in the ODE (13), we can find that a set of parametric resonances at $\Omega_{12} \simeq 2\Omega_1,\; 2\Omega_2$ exist. This follows directly from the fact that we then have two uncoupled Mathieu equations [34] in the variables ξ_+ and ξ_-. Note that resonances at low $(2\Omega_1)$ and high $(2\Omega_2)$ frequencies occur [see Eq. (11)].

Numerical solutions of the ODE model (13) are presented in Fig. 1 for parameters corresponding to the BCS regime. It is found that amplitudes are growing exponentially in time and the behavior agrees well with the theoretical predictions. Using the same parameters, we perform numerical simulations of the full PDE model (1) describing the Fermi-Bose mixture, see Fig. 2. Results shows quantitative agreement for the PDE and ODE models upto $t \sim 10$. From Fig. 3, where data for the spatial wavelength L of the FW versus the modulation

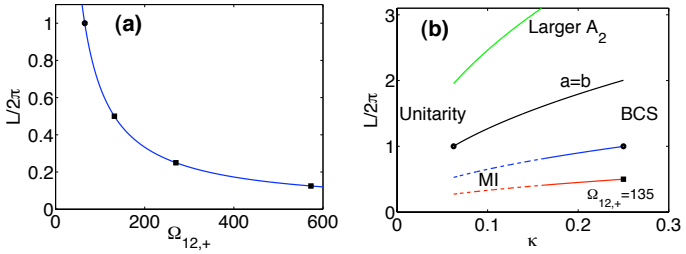

FIG. 3: (Color online) Spatial wavelengths of the Faraday patterns. In (a) we use parameters as for Fig. 1 with the left dot ($k = 1$) corresponding to $\Omega_{12,+} = 65.5$. In (b) the case corresponding to Fig. 1 (right dot) is the second (blue) curve from the bottom. Here, as well as for the lowest (red) curve [left square in (a)] where $\Omega_{12,+} = 135$ ($k = 2$), the condition (12) is not fulfilled in the entire domain, hence MI is possible in the left part (dashed lines). The condition (12) for not having MI can be satisfied in the entire κ range, e.g. by choosing $A_2 = 2 \cdot \sqrt{20}$ larger, top (green) curve. Finally, the special case of $a = b$ (i.e. with $g_b^{(0)} \propto \kappa$) is illustrated with the third (black) curve, where the left dot corresponds to the case illustrated in Fig. 4.

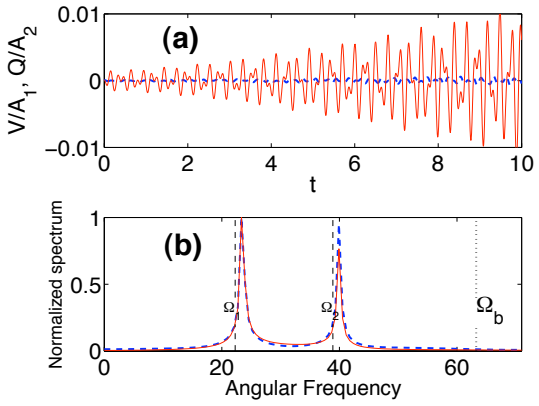

FIG. 4: (Color online) Solutions to the ODE model of Eq. (14). (a) Amplitudes growing exponentially in time. (b) Spectrum for the modulation frequency $\Omega_b = 63.3$ ($k = 1$) and with Ω_1 and Ω_2 agreeing well with (11) in this regime. Same initial conditions as in Fig. 1, while the parameters here are: $\alpha_b = 0.25$, $A_1 = \sqrt{5000}$, $A_2 = \sqrt{20.2}$, $g_b^{(0)} = 0.1$, $g_{12}^{(0)} = 0.8$ and $\kappa = 1/16$.

frequency are plotted in (a), it is seen how the wavelength is decreasing when the frequency is growing. While results for the wavenumber $k = 1$ have been presented in Figs. 1 and 2, we have numerically confirmed the results for $k = 2, 3, 4$ [squares in Fig. 3 (a)] also with full PDE simulations. In Fig. 3 (b) we show how L depends on the fermionic subsystem parameter κ within the analytic model (18).

The results of Eq. (19) in practice here means that with the parameter values of Fig. 1 the modulation frequency can be in the order of 1% larger (or smaller) when exciting the FW. This have been confirmed numerically with Eqs. (1) and (13), and we have also observed a weak dependence on α_{12} for the maximum of the Ω_{12} resonance region. Hence, by optimizing Ω_{12} a larger amplitude can be obtained [i.e. the numerical curve (A) in Fig. 6 can be moved further towards the line of the maximal theoretical gain].

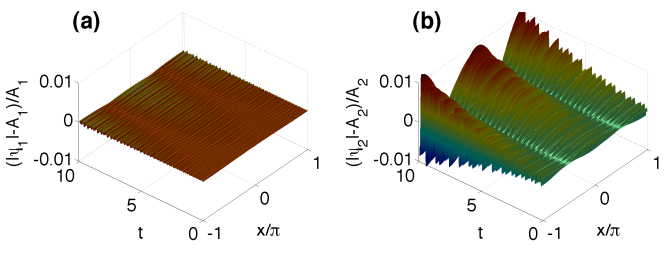

FIG. 5: (Color online) Solutions to the full PDE model of Eq. (1) for driven nonlinearity for bosons with the modulation frequency $\Omega_b = 63.3$ ($k = 1$). Same initial and boundary conditions as in Fig. 2, while the parameters are the same as for Fig. 4

B. Driven nonlinearity in the bosonic subsystem

The case where only the intra-spieces (boson-boson) interaction parameter is modulated is described by the system (14). Applying again the multiscale approach (see the Appendix), we have concluded that resonances occurs at $\Omega_b = 2\omega_1$ under the additional condition that $\omega_1 \simeq \omega_2$. Hence, from Eq. (8) with $\omega_1 = \omega_2$ we now obtain

$$\Omega_b = 2k\sqrt{k^2 + a}, \quad k^2 = \frac{a}{2}\left(\sqrt{1 + \Omega_b^2/a^2} - 1\right). \qquad (21)$$

The corresponding instability region is bounded by the lines

$$\bar{\omega}_1^2 = \omega_1^2 \pm \frac{\varepsilon_0 \alpha_b}{2}, \ \bar{\omega}_2 = \bar{\omega}_1, \qquad (22)$$

and the maximal gain is now equal to

$$p_m \simeq \frac{\varepsilon_0 \alpha_b}{4\omega_1}. \qquad (23)$$

Numerical solutions of the ODE model (14) with exponentially growing amplitudes are presented in Fig. 4 for parameters corresponding to the molecular unitarity limit. In the spectrum we can see peaks corresponding to the combination of two excited frequencies for both components. These predictions are again well confirmed by PDE simulations of the system (1) with driven nonlinearity of bosons, see Fig. 5. Although the bosonic component ψ_1 is lagging behind (i.e. lower amplitude in Figs. 4 and 5) it is growing exponentially with the same rate as ψ_2.

According to Eq. (22) the modulation frequency can be in the order of 3% larger or smaller (for the parameters

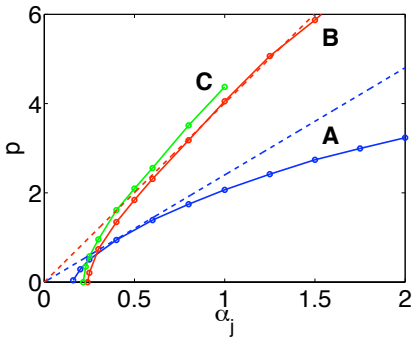

FIG. 6: (Color online) Exponential growth rates p of the slowly varying amplitudes [envelope of $V \sim Q \sim \exp(pt)$ of (7)]. Solid curves shows numerical data (dots) for the three cases: A (Fermi-Bose modulation, $\alpha_j = \alpha_{12}$), B (Bose-Bose modulation, $\alpha_j = \alpha_b$) and C (Super-resonance, $\alpha_j = \alpha_b = -\alpha_{12}$). Dashed lines shows theoretical predictions according to Eq. (20) for case A, and Eq. (23) for case B. In case A, $\Omega_{12} = 65.5$, while in cases B (C) we use $\Omega_b = 63.3$ $(= \Omega_{12})$.

of Fig. 4) when exciting the FW. This have been confirmed numerically with Eqs. (1) and (14), although the numerical resonance region was found for slightly lower values of Ω_b than the theoretical estimate.

Finally we can analyse also this case in terms of the (anti-) symmetric combinations $\xi_\pm$. From Eq. (14) we then have the driven coupled Mathieu-like system

$$\xi_{\pm,tt} + \Omega_{1,2}^2 \xi_\pm + \alpha_b \omega_1^2 \cos(\Omega_b t)[\xi_+ + \xi_-]/2 = 0, \quad (24)$$

and in agreement with our findings above, the literature here states that $\Omega_b \simeq 2\Omega_1,\ 2\Omega_2$ and $\Omega_1 + \Omega_2$ in this case, see e.g. [11, 33].

C. Driven super-resonance

Comparing (16) with (21), we note that when $a = b$, we have $\Omega_{12,+} = \Omega_b$. Now we change a sign in Eq. (2), such that for example for $\alpha_{12} = -\alpha_b$, then the two types of modulations initiate opposite phases for the two components and an increased growth rate of the Faraday waves are observed, as compared to the two distinct cases discussed before. For demonstrating super-resonance numerically we used the parameters as for Fig. 4 with $\alpha_{12} = -0.25$. Also this result can be understood from a consideration of the system (7) for symmetric and antisymmetric combinations, ξ_+ and ξ_-. For example in the case when $\alpha_{12} = -\alpha_b/2$ and $\Omega_{12} = \Omega_b$, we simply have the driven coupled Mathieu-like system

$$\xi_{\pm,tt} + [\Omega_{1,2}^2 + \Omega_{2,1}^2 \frac{\alpha_b}{2} \cos(\Omega_b t)]\xi_\pm = -\omega_1^2 \frac{\alpha_b}{2} \cos(\Omega_b t)\xi_\mp. \quad (25)$$

V. GROWTH RATES OF THE FW

In general we note, that in the regime where the linear stability analysis based on Eqs. (5) and (6) are valid we have quantitative agreement between the full model (1), see Figs. 2 and 5, and the ODE models (13) and (14), Fig. 1 respectively Fig. 4. We found an exponential growth in time of the oscillating amplitudes in this regime. For larger times the nonlinearities of the full model (1) cause a saturation of the amplitudes, while the results of the linear stability analyse becomes unphysical.

In Fig. 6 we show results of the exponential growth rate for the three sections A, B and C above, together with the theoretical results for the maximal gain derived in the Appendix. We show results only for the wavenumber $k = 1$, however, we note that the theoretical estimates $p_m(k)$ are increasing with k and are asymptotically approaching the constant $\lim_{k\to\infty} p_m(k) = \alpha_j g_{12}^{(0)} A_1 A_2/2$.

VI. CONCLUSION

In conclusion we have illustrated the possibility of Faraday patterns for Fermi-Bose mixtures, i.e. with atomic bosons coupled to fermions, both in the fermionic BCS regime and in the molecular unitarity limit. In particular we have investigated quasi-one-dimensional superfluid FB mixtures with periodic variations in time of the Fermi-Bose or Bose-Bose interactions. We find Faraday patterns for both cases and study their properties depending on the parameters for modulations and of the system settings. Combining the two types of modulations can results in even larger amplitudes.

We also conjecture that Faraday waves can be observed in an atomic BEC coupled to a Tonks-Girardeau gas.

A natural continuation of this work is to investigate Faraday patterns in FB mixtures for the 2D and 3D cases. This problem reserves a separate investigation though, since the corresponding coupled nonlinear-Schrödinger-like equations are different.

Acknowledgements

F. Kh. A. acknowledge partial support from the Fundacao de Amparo a Pesquisa do Estado de Sao Paulo (FAPESP) Brasil, and the appointment as Otto Mønsted Guest Professor at DTU.

Appendix

To understand the resonances in the coupled system (13), we can use the multiscale analysis [32]. Following this approach, we look for solutions where

$$\omega_1^2 = \omega_{01}^2 + \varepsilon_0 a_1 + \varepsilon_0^2 a_2 + ...,\ \omega_2^2 = \omega_{02}^2 + \varepsilon_0 b_1 + \varepsilon_0^2 b_2 + ..., \quad (26)$$

and correspondingly for the functions V and Q

$$\begin{aligned} V &= V_0(t,T) + \varepsilon_0 V_1(t,T) + \varepsilon_0^2 V_2(t,T) + ..., \\ Q &= Q_0(t,T) + \varepsilon_0 Q_1(t,T) + \varepsilon_0^2 Q_2(t,T) + ..., \end{aligned} \quad (27)$$

where $T = \varepsilon_0 t$ is a slow time. Taking the terms of each order in ε_0 we obtain from (13) the following system of equations up to the linear order in ε_0

$$\begin{aligned} V_{0,tt} + \omega_{01}^2 V_0 &= 0, \quad Q_{0,tt} + \omega_{02}^2 Q_0 = 0, \quad (28) \\ V_{1,tt} + \omega_{01}^2 V_1 &= -2V_{0,tT} - a_1 V_0 + [1 + \alpha_{12}\cos(\Omega t)]\, Q_0, \\ Q_{1,tt} + \omega_{02}^2 Q_1 &= -2Q_{0,tT} - b_1 Q_0 + [1 + \alpha_{12}\cos(\Omega t)]\, V_0. \end{aligned}$$

The solutions of the two upper uncoupled equations in (28) can be written in the form

$$\begin{aligned} V_0(t,T) &= A_0(T)\cos(\omega_{01}t) + B_0(T)\sin(\omega_{01}t), \\ Q_0(t,T) &= C_0(T)\cos(\omega_{02}t) + D_0(T)\sin(\omega_{02}t). \end{aligned} \quad (29)$$

Then we require the absence of the resonant terms in the right hand side of the two lower equations in (28). With the ansatz $\Omega = \omega_2 \pm \omega_1$, and after averaging in the fast time t, we obtain a system of equations for the envelope functions A_0, B_0, C_0 and D_0 of (29)

$$\begin{aligned} 2\omega_{01}A_{0,T} - a_1 B_0 \mp \frac{\alpha_{12}}{2} D_0 = 0, \\ -2\omega_{01}B_{0,T} - a_1 A_0 + \frac{\alpha_{12}}{2} C_0 = 0, \\ 2\omega_{02}C_{0,T} - b_1 D_0 \mp \frac{\alpha_{12}}{2} B_0 = 0, \\ -2\omega_{02}D_{0,T} - b_1 C_0 + \frac{\alpha_{12}}{2} A_0 = 0. \end{aligned} \quad (30)$$

Looking for solutions of the form $A_0, B_0, C_0, D_0 \sim \exp(pt)$, i.e. (for example) with $A_{0,T} \sim pA_0/\varepsilon_0$, we find from (30) the characteristic equation $p^4 + Mp^2 + N = 0$ with coefficients

$$M = \frac{2b_1^2\omega_{01}^2 + 2a_1^2\omega_{02}^2 \mp \alpha_{12}^2\omega_{01}\omega_{02}}{8\omega_{01}^2\omega_{02}^2}, N = \frac{(4a_1b_1 - \alpha_{12}^2)^2}{256\omega_{01}^2\omega_{02}^2}. \quad (31)$$

Remember that the sign $\mp$ in M of (31) is for $\Omega_{12,\pm} = \omega_2 \pm \omega_1$ respectively, and note also that $N \geq 0$. Hence, from $p^2 = -M/2 \pm \sqrt{M^2/4 - N}$ it is seen that only $\Omega_{12,+}$ can correspond to a positive real p, i.e. a FW with an exponentially growing amplitude, while excitations for $\Omega_{12,-}$ are stable.

The maximal exponential growth rate of the FW for $\Omega_{12,+}$ is found from (31) with $M^2 \sim 4N$ to be

$$p_m \sim \sqrt{-\frac{M}{2}} \simeq \frac{\varepsilon_0\alpha_{12}}{4\sqrt{\omega_1\omega_2}}, \quad (32)$$

which is refered to as the theoretical gain in the main text.

For experiments on FW it is important to know also the width of the instability regions. The boundaries of the unstable region can be found from inspection of Eq. (31), which shows that at the boundary we have from N that $b_1 = \alpha_{12}^2/(4a_1)$ and correspondingly from M we then have $a_1 = \pm\frac{\alpha_{12}}{2}\sqrt{\omega_1/\omega_2}$, such that the frequences to linear order in ε_0 obtained from (26) are

$$\omega_1^2 = \omega_{01}^2 \pm \varepsilon_0 \frac{\alpha_{12}}{2}\sqrt{\frac{\omega_1}{\omega_2}} + ..., \; \omega_2^2 = \omega_{02}^2 \pm \varepsilon_0 \frac{\alpha_{12}}{2}\sqrt{\frac{\omega_2}{\omega_1}} + ... \quad (33)$$

Analogously the system (14) for the case of driven boson-boson interactions can be investigated and the results are reported in Eqs. (21), (22) and (23) in the main text. Below we sketch the derivation also for this case.

For $\varepsilon_0 = 0$ the upper equation in (14) is a Mathieu equation

$$V_{tt} + [\omega_1^2 + \alpha_b\omega_1^2\cos(\Omega t)]V = 0, \quad (34)$$

with solutions $V = A\,\mathrm{Ce}(a,q,t) + B\,\mathrm{Se}(a,q,t)$, where $a = 4\omega_1^2/\Omega^2$ and $q = -2\alpha_b\omega_1^2/\Omega^2$ in the standard notation of the cosine- and sine Mathieu functions [34]. We now look again for solutions to (14) of the form of Eqs. (26) and (27). In the case of $\alpha_b \ll 1$ one can use the expansions $\mathrm{Ce}(a,q,t) \sim \cos(\omega_{01}t) + \mathcal{O}(q)$ and $\mathrm{Se}(a,q,t) \sim \sin(\omega_{01}t) + \mathcal{O}(q)$ in Eq. (34). In particular we then have that the system in the upper equations of (28), and hence (29), applies also here and we have in the linear order

$$\begin{aligned} V_{1,tt} + \omega_{01}^2 V_1 &= -2V_{0,tT} - a_1 V_0 - \alpha_b\cos(\Omega t)V_0 + \varepsilon_0 Q_0, \\ Q_{1,tt} + \omega_{02}^2 Q_1 &= -2Q_{0,tT} - b_1 Q_0 + \varepsilon_0 V_0. \end{aligned} \quad (35)$$

Hence, A_0 and B_0 are not coupled to C_0 and D_0 in the lowest order in ε_0, such that it is enough to consider the two envelope functions A_0 and B_0 in the remainder. We then require the absence of the resonant terms in the right hand side of the upper equation in (35). With the ansatz $\Omega = 2\omega_1$ and $\omega_2 = \omega_1$ ($b_1 = a_1$), we obtain a system of equations for A_0 (with $A_{0,T} \sim pA_0/\varepsilon_0$) and B_0 such that the characteristic equation give

$$p = \pm\frac{\varepsilon_0}{2\omega_1}\sqrt{\frac{\alpha_b^2}{4} - a_1^2}. \quad (36)$$

Hence the theoretical gain for $a_1 \sim 0$ is

$$p_m = \frac{\varepsilon_0\alpha_b}{4\omega_1}. \quad (37)$$

Since p becomes imaginary when $a_1^2 > \alpha_b^2/4$, we have the boundary $a_1 = b_1 = \pm\alpha_b/2$ and hence $\omega_1^2 = \omega_2^2 \simeq \omega_{01}^2 \pm \varepsilon_0\frac{\alpha_b}{2}$.

[1] M. Faraday, Philos. Trans. R. Soc. London **121**, 319 (1831).

[2] F. Matera, A. Mecozzi, M. Romagnoli, and M. Settembre, Opt. Lett. **18**, 1499 (1993).

[3] F. Kh. Abdullaev, Pisma JTP, **20**, 25 (1994) (in Russian).

[4] F. Kh. Abdullaev, S. A. Darmanyan, S. Bishoff, M. P. Sørensen, J. Opt. Soc. Am. B **14**, 27 (1997).

[5] F. Kh. Abdullaev, S. A. Darmanyan, and J. Garnier, *Modulational instability of electromagnetic waves in inhomogeneous and discrete systems*, in Progress in Optics, **44**, 306 (2002).

[6] A. Armaroli, F. Biancalana, arXiv:1208.3484v1.

[7] M. Droques et al. in CLEO: "Science and Innovations" (OSA, 2012) p.CTh4B.7.

[8] K. Staliunas, S. Longhi and G. J. de Valcárcel, Phys. Rev. Lett. **89**, 210406 , (2002).

[9] K. Staliunas, S. Longhi and G. J. de Valcárcel, Phys. Rev. A **70**, 011601 (2004).

[10] A. I. Nicolin, R. Carretero-Gonzalez, and P. G. Kevrekidis, Phys. Rev. A **76**, 063609 (2007).

[11] A. B. Bhattacherjee, Phys. Scr. **78**, 045009 (2008).

[12] A. Balaz, and A. I. Nicolin, Phys. Rev. A **85**, 023613 (2012).

[13] R. Nath and L. Santos, Phys. Rev. A **81**, 033626 (2010).

[14] K. Lakomy, N. Nath, and L. Santos, Phys. Rev. A **86**, 023620 (2012).

[15] P. Engels, C. Antherton and M. A. Hoefer, Phys. Rev. Lett. **98**, 095301, (2007).

[16] P. Capuzzi, P. Vignolo, Phys. Rev. A **78**, 043613 (2008).

[17] R. A. Tang, H. C. Li and J. K. Hue, J. Phys. B **44**, 115303 (2011).

[18] Yu. Kagan, E. L. Surkov, and G. V. Shlyapnikov, Phys. Rev. A **54**, R1753 (1996).

[19] Yu. Kagan, L. A. Manakova, Phys. Rev. A **76**, 023601 (2007).

[20] S. Inouye, M. R. Andrews, J. Stenger, H.-J. Miesner, D. M. Stamper-Kurn and W. Ketterle, Nature (London) **392**, 151 (1998).

[21] H. Saito and M. Ueda, Phys. Rev. Lett. **90**, 040403 (2003); F. Kh. Abdullaev, A. M. Kamchatnov, V. V. Konotop and V. A. Brazhnyi, Phys. Rev. Lett. **90**, 230402 (2003); D. E. Pelinovsky, P. G. Kevrekidis and D. J. Frantzeskakis, Phys. Rev. Lett. **91**, 240201, (2003); F. Kh. Abdullaev, J. G. Caputo, R. A. Kraenkel and B. A. Malomed, Phys. Rev. A **67**, 013605 (2003).

[22] P. Capuzzi, M. Gattobigio, and P. Vignolo, Phys. Rev. A **83**, 013603 (2012).

[23] S. K. Adhikari and L. Salasnich, Phys. Rev. A **76**, 023612 (2007); Phys. Rev. A **77**, 033618 (2008); Phys. Rev. A **78**, 043616 (2008).

[24] L. Tonks, Phys. Rev. **50**, 955 (1936); M. Girardeau, J. Math. Phys. (N.Y.) **1**, 516 (1960).

[25] E. B. Kolomeisky, T. J. Newman, J. P. Straley and X. Qi, Phys. Rev. Lett. **85**, 1146 (2000); M. Ögren, G. M. Kavoulakis and A. D. Jackson, Phys. Rev. A **72**, 021603(R) (2005).

[26] H. Heiselberg, Phys. Rev. Lett. **93**, 040402 (2004); **108**, 249904(E) (2012).

[27] A. Bulgac and G. F. Bertsch, Phys. Rev. Lett. **94**, 070401 (2005).

[28] N. Manini and L. Salasnich, Phys. Rev. A **71**, 033625 (2005).

[29] G. E. Astrakharchik, R. Combescot, X. Leyronas, and S. Stringari, Phys. Rev. Lett. **95**, 030404 (2005); G. E. Astrakharchik, J. Boronat, J. Casulleras, and S. Giorgini, Phys. Rev. Lett. **93**, 200404 (2004).

[30] S. Adhikari, Phys. Rev. A **77**, 045602 (2008).

[31] A. H. Nayfeh, *Introduction to Perturbation Techniques*, WILEY-VCH p. 253 (1981).

[32] G. M. Makhmoud, Physica A **242**, 239 (1997).

[33] J. Hansen, Ing.-Archiv **55**, 463 (1985).

[34] M. Abramowitz and I. A. Stegun, *Handbook of Mathematical Functions with Formulas, Graphs, and Mathematical Tables*, Dover N.Y. (1972).